Published in final edited form as:

Angew Chem Int Ed Engl. 2016 September 12; 55(38): 11577–11581. doi:10.1002/anie.201606242.

A Panel of TrpB Biocatalysts Derived from Tryptophan Synthase through the Transfer of Mutations that Mimic Allosteric Activation

Javier Murciano-Calles[a,b], **David K. Romney**[a,b], **Sabine Brinkmann-Chen**[a], **Andrew R. Buller**[a], and **Frances H. Arnold**[a,*]

[a]Division of Chemistry and Chemical Engineering, California Institute of Technology, Pasadena, California 91125, USA

Abstract

Naturally occurring enzyme homologs often display highly divergent activity with non-natural substrates. Exploiting this diversity with enzymes engineered for new or altered function, however, is laborious because the engineering must be replicated for each homolog. We demonstrate that a small set of mutations of the tryptophan synthase β-subunit (TrpB) from *Pyrococcus furiosus*, which mimic the activation afforded by binding of the α-subunit, has a similar activating effect in TrpB homologs with as little as 57% sequence identity. Kinetic and spectroscopic analyses indicate that the mutations function through the same mechanism, mimicry of α-subunit binding. From this collection of stand-alone enzymes, we identified a new catalyst that displays a remarkably broad activity profile in the synthesis of 5-substituted tryptophans, a biologically important class of compounds. This investigation demonstrates how allosteric activation can be recapitulated throughout a protein family to efficiently explore natural sequence diversity for desirable biocatalytic transformations.

TOC image

The tryptophan synthase enzyme complex is active toward a number of indole analogs. The β-subunit (TrpB) performs the synthetically useful reaction, but requires the α-subunit to be fully active. We have transferred mutations from a re-activated TrpB variant from *Pyrococcus furiosus* into homologous TrpBs to generate a panel of stand-alone TrpB catalysts, one of which is especially useful for making 5-substituted tryptophans, an important biological motif.

* frances@cheme.caltech.edu.

[b]These authors contributed equally to this work.

Supporting information for this article is given via a link at the end of the document.

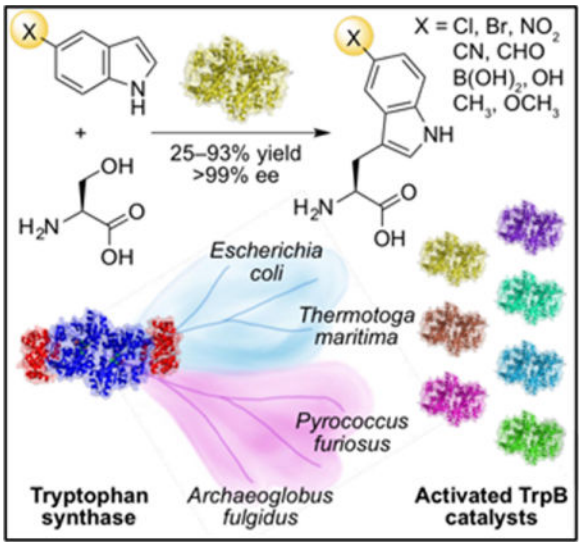

Keywords

allostery; protein engineering; tryptophan synthase; non-canonical amino acids; biocatalysis

Tryptophan synthases (TrpSs) are $\alpha_2\beta_2$ heterodimer complexes that catalyze the synthesis of tryptophan (**1**) from 3-indole-D-glycerol phosphate (IGP, **2**) and L-serine (**3**, Figure 1a). TrpS also reacts with myriad indole analogs, providing a direct biocatalytic route to making tryptophan derivatives.[1] In such reactions, only the β-subunit (TrpB) performs catalysis (Figure 1b), but its activity is greatly diminished in the absence of the α-subunit (TrpA), limiting its utility as a biocatalyst.[2] Recently, we applied directed evolution to the β-subunit from *Pyrococcus furiosus* (*Pf*TrpB) to identify mutations that emulate the effect of TrpA binding and imbue the β-subunit with high activity in isolation.[3] However, this stand-alone catalyst, *Pf*TrpB^{0B2}, exhibited poor levels of activity in the synthesis of 5-substituted tryptophans, a prevalent structural motif in bioactive natural products.[4] We hypothesized that if TrpB homologs could be activated by transferring the allostery-mimicking mutations identified in *Pf*TrpB^{0B2}, some of the resultant catalysts might have greater activity with 5-substituted indoles.

The central challenge in enzyme engineering is to traverse the sequence space that separates a wild-type enzyme from its variant with novel functional properties. Instead of repeating the directed evolution to activate each new TrpB homolog, we decided to try to shortcut that effort by transferring beneficial mutations discovered in *Pf*TrpB to different homologs. This would create a panel of TrpB enzymes, possibly with different substrate scopes or other useful properties for biocatalytic applications. Transfer of beneficial mutations to other, closely-related enzymes is widely used to improve properties, such as stability, but this approach assumes either that the effects of the mutations are independent and additive, as with thermostabilization by consensus design,[5] or at least that the protein context is shared (high sequence identity in the region of the mutation).[6] In an allosterically modulated enzyme such as TrpS, catalytic activity is increased by ligand (TrpA) binding at a location separate from the active site. Allosteric activation thus involves the participation of many

residues, even the entire protein, as well as the surrounding solvent.[7] Furthermore, residues that contribute to allosteric signalling are poorly conserved by evolution,[8] causing homologous proteins to develop different allosteric mechanisms.[9] It was thus uncertain whether mutations that mimic allostery in TrpS from one species would be generalizable to other homologs.

We selected three phylogenetically diverse TrpBs[10] to serve as the basis for new stand-alone catalysts: the hyperthermostable enzymes from *Archaeoglobus fulgidus* (*Af*TrpB, 72% sequence identity to *Pf*TrpB) and *Thermotoga maritima* (*Tm*TrpB, 64% identity), and the mesophilic enzyme from *Escherichia coli* (*Ec*TrpB, 57% identity).[11] We were especially interested in *Tm*TrpB because its wild-type k_{cat} is already four times that of *Pf*TrpB.[12] Activation of *Ec*TrpB would be desirable because it is adapted to a different temperature (37 °C *versus* 96 °C for *Pf*TrpB), which may be useful for less stable substrates.

Previously, we observed that *Pf*TrpB was a sluggish catalyst (Table 1, entry 1), but that variant *Pf*TrpB^{0B2}, which was engineered using three rounds of directed evolution, exhibited a 9-fold increase in k_{cat} with an equivalent decrease in K_M (Table 1, entry 2). We expressed and purified the three TrpB homologs and their corresponding 0B2 variants to test whether the activating mutations would produce a similar effect. Compared to *Af*TrpB (Table 1, entry 3), the variant *Af*TrpB^{0B2} has a 7-fold higher k_{cat} and 2-fold lower K_M for indole (Table 1, entry 4).

The absorption spectrum of PLP changes as the cofactor passes through different states of the catalytic cycle (Figure 1b).[2a] Thus, the absorption spectrum of the enzyme under reaction conditions directly reflects the steady-state distribution of catalytic intermediates. Before the addition of Ser, *Af*TrpS, *Af*TrpB, and *Af*TrpB^{0B2} all display an absorbance peak at 412 nm (Figure 2), which corresponds to the absorbance of E(A_{in}). When Ser is added to *Af*TrpS, its spectrum exhibits a new λ_{max} at 350 nm (Figure 2a), indicating that E(A-A) is prevalent in the steady state of the catalytic cycle for this enzyme. Conversely, *Af*TrpB lacks a λ_{max} at 350 nm, but instead possesses an absorbance peak at 428 nm (Figure 2b), indicating that E(Aex_1) is the most prevalent intermediate. The spectrum of *Af*TrpB^{0B2}, on the other hand, is almost identical to that of *Af*TrpS, with a prominent λ_{max} of 350 nm (Figure 2c). This behavior matches what we observed previously[3] and provides compelling evidence that the 0B2 mutations activate *Af*TrpB by the same mechanism as they did in *Pf*TrpB, namely by mimicking the allosteric activation produced by binding of TrpA to TrpB.

The *Tm*TrpB homolog (Table 2, entry 1) already contains the residue A321 in its native sequence. However, incorporation of the remaining five mutations from *Pf*TrpB^{0B2} reduced the k_{cat} to just 10% of the wild-type activity (Table 2, entry 2). To investigate whether a subset of these mutations could still be activating, we constructed a recombination library of the 0B2 mutations in *Tm*TrpB and screened for activity with indole. Three mutations, P19G, I69V, and T292S, increased the activity with respect to wild type. The variant having all three mutations was most active, with an 8-fold increase in k_{cat} (Table 2, entry 3). The T292S mutation by itself was also substantially activating, producing a 4-fold increase in k_{cat} (Table 2, entry 4).

As with *Af*TrpS and *Pf*TrpS, the UV-vis absorption spectrum of *Tm*TrpS exhibits a strong λ_{max} at 350 nm under the reaction conditions. Once again, *Tm*TrpB lacks this probative peak and instead exhibits the λ_{max} at 428 nm that was observed for *Af*TrpB and *Pf*TrpB. While all permutations of the three mutations (P19G, I69V, and T292S) led to improved k_{cat} values (Figure S3), only the variants with T292S exhibited a λ_{max} at 350 nm, equivalent to *Tm*TrpS (Figure S4). The importance of the T292S mutation was also observed in *Pf*TrpB, where this mutation alone restored the k_{cat} of the isolated *Pf*TrpB to that of the *Pf*TrpS complex[3]. The effects of this conservative mutation were even more dramatic in *Tm*TrpB, producing a k_{cat} almost 3-fold higher than *Tm*TrpS (Table 2, *cf.* entries 4 and 5).

Mutational activation of the most distant homolog, *Ec*TrpB (57% identity), proved more challenging. The crucial Thr→Ser mutation was not possible for *Ec*TrpB because *Ec*TrpB already has Ser at this position (S297). Site-saturation mutagenesis confirmed that serine is the optimal residue at that position (Figure S5a). Unlike *Tm*TrpB, recombination of the 0B2 mutations in *Ec*TrpB yielded no variants with enhanced activity and only a few with activity similar to wild type (Figure S5b).

The initial screening effort with *Pf*TrpB[3] had also identified a variant with mutations M144T and N166D that was almost as active as *Pf*TrpB^{T292S} (Table 3, entry 1). These two residues, unlike T292, reside in the so-called communication (COMM)[2a] domain, which interfaces with TrpA and undergoes large conformational motions during the catalytic cycle. These residues are identical in the four homologs studied here and are almost universally conserved across all TrpBs (Figure S6). We hypothesized that the effects of mutations at these sites might also be transferrable. Upon making the equivalent mutations in *Ec*TrpB, *Tm*TrpB, and *Af*TrpB, we observed activation in all variants, with approximately 2- to 5-fold increases in k_{cat} (Table 3, entries 2 to 4).

We wished to verify that the proteins were still being activated by allosteric mimicry. UV-vis analysis of the steady-state distributions of intermediates upon addition of L-serine revealed that the double mutants of *Pf*TrpB and *Ec*TrpB still accumulated E(Aex_1) rather than E(A-A) (Figure S7a and d). However, the homologous double mutants of *A. fulgidus* and *T. maritima* showed shifted spectra, in which E(A-A) predominated (Figure S7b and c). These data suggest that the double mutation is also activating the enzymes through allosteric mimicry, but that it does not quite reach the activation generated by adding TrpA. This situation is reminiscent of the earlier evolution of *Pf*Trp^{0B2}, wherein the lone T292S mutation was insufficient to completely shift the UV-vis spectrum to E(A-A) without at least four additional mutations.[3]

In the pantheon of tryptophan-derived natural products, one can find substitution at every position on the indole moiety (Figure 3). Position 5, for example, is chlorinated by the halogenase PyrH, *en route* to pyrroindomycin B (**6**),[4a] and mono-oxygenated by tryptophan hydroxylase in the biosynthesis of serotonin (**7**) and melatonin (**8**).[4d] Such substituents have a profound effect on biological activity because they can mask sites of metabolic degradation and change the compound's electronic properties. This, in turn, alters properties like solubility and creates new binding interactions through effects such as π-stacking and halogen bonding.[1b, 13] Halogens can also provide handles for further diversification of

biologically active compounds through cross-coupling reactions.[14] While biocatalytic routes to tryptophan derivatives tend to be inefficient and limited in substrate scope, TrpS can provide direct access to many of these products. Previously, however, 5-substituted indoles bearing anything larger than fluorine caused a substantial decrease in activity[1d, 1f, 15]. Furthermore, TrpS activity with electron-deficient indoles had not been explored.

One enzyme in our repertoire, *Tm*TrpB$^{M145T\ N167D}$, showed higher activity with 5-bromoindole than even our most optimized catalyst, *Pf*TrpB^{0B2} (Figure S8). To assess whether this was a general property of the catalyst, we compared the relative rates of *Tm*TrpB$^{M145T\ N167D}$ to *Pf*TrpB^{0B2} with a set of challenging 5-substituted indoles (Table 4). We then applied *Tm*TrpB$^{M145T\ N167D}$ in reactions that were run to higher conversion in order to isolate and characterize the products.

With 5-chloroindole, the *Tm* variant exhibits a 3-fold rate enhancement compared to *Pf*TrpB^{0B2} (Table 4, entry 1). Despite this improvement, the reaction still appeared to stall at about 85% conversion when the substrates were used in equal amounts, possibly due to competing decomposition of serine.[16] We overcame this limitation by using a small excess of serine, allowing us to obtain 5-chlorotryptophan in 94% isolated yield. *Pf*TrpB^{0B2} has even greater difficulty with 5-bromoindole, but the *Tm* variant is almost six times as fast for this substrate, allowing us to obtain 5-bromotryptophan in 88% isolated yield (Table 4, entry 2). These results compare favorably with previous reports, in which TrpS from *Salmonella enterica* was shown to form 5-chloro and 5-bromotryptophan in 61% and 26% yield, respectively[1f].

*Tm*TrpB$^{M145T\ N167D}$ exhibits substantially faster rates, ranging from 2- to over 7-fold, with substrates that bear electron-withdrawing groups, such as nitro, cyano, formyl, and even boronate (Table 4, entries 3–6), representing a new substrate class in the TrpS literature. The reaction with 5-boronoindole is particularly interesting, as the catalyst must contend with competing proto-deborylation. Boronic acids can serve as handles for bio-orthogonal conjugation,[17] pH-sensitive delivery of therapeutics *in vivo*,[18] and substrates for cross-coupling, complementing 5-halotryptophans, for which electron-deficient coupling partners lead to reduced yields.[19] Although the reactivity with these new substrates remains low, we believe that *Tm*TrpB$^{M145T\ N167D}$, which only has two mutations compared to six in *Pf*TrpB^{0B2}, is the ideal parent for further optimization.

*Pf*TrpB^{0B2} already has excellent activity with substrates that bear electron-donating groups at the 5-position (e.g., hydroxy, methyl, and methoxy); nonetheless, *Tm*TrpB$^{M145T\ N167D}$ delivers a 1.5-fold faster rate (Table 4, entries 7–9), which is helpful because such electron-rich substrates are prone to aerobic oxidation. Thus, *Tm*TrpB$^{M145T\ N167D}$ performs almost 10,000 turnovers in just two hours, allowing the products to be isolated in high yield without the need for oxygen-free conditions.

By mining the wealth of activating mutations in *Pf*TrpB, we have identified subsets that retain their effects when transferred into related enzymes, including those from different domains of life (*archaea* and bacteria). Importantly, spectroscopic data indicate that the

homologs are activated through the same mechanism as the *Pf*TrpB variants, namely mimicking the effects of TrpA binding. By screening the resulting panel of activated TrpB homologs, we have identified a variant with broadly improved activity toward 5-substituted indoles, a substrate class that had proven problematic for all previous catalysts. The strategy used here could be applied to other TrpBs and exemplifies how the transfer of activating mutations to homologous enzymes can rapidly expand activity with non-native substrates.

Supplementary Material

Refer to Web version on PubMed Central for supplementary material.

Acknowledgments

The authors thank Dr. Jackson Cahn for the data on frequency of amino acids in each position of TrpB and Dr. Jennifer Kan for helpful discussions and comments on the manuscript. J.M.-C. gratefully acknowledges support from the Alfonso Martín Escudero Foundation. This work was funded through the Jacobs Institute for Molecular Engineering for Medicine and Ruth Kirschstein NIH Postdoctoral Fellowships F32GM117635 (to D.K.R) and F32G110851 (to A.R.B.).

References

1. a) Ferrari D, Yang LH, Miles EW, Dunn MF. Biochem. 2001; 40:7421–7432. [PubMed: 11412095] b) Goss RJM, Newill PLA. Chem Comm. 2006:4924–4025. [PubMed: 17136248] c) Winn M, Roy AD, Grüschow S, Parameswaran RS, Goss RJM. Bioorg Med Chem Lett. 2008; 18:4508–4510. [PubMed: 18667314] d) Tsoligkas AN, Winn M, Bowen J, Overton TW, Simmons MJH, Goss RJM. ChemBioChem. 2011; 12:1391–1395. [PubMed: 21608096] e) Perni S, Hackett L, Goss RJ, Simmons MJ, Overton TW. AMB Express. 2013; 3:66–75. [PubMed: 24188712] f) Smith DRM, Willemse T, Gkotsi DS, Schepens W, Maes BUW, Ballet S, Goss RJM. Org Lett. 2014; 16:2622–2625. [PubMed: 24805161] g) Corr MJ, Smith DRM, Goss RJM. Tetrahedron. 2016; doi: 10.1016/j.tet.2016.02.016
2. a) Dunn MF. Arch Biochem Bioph. 2012; 519:154–166.b) Niks D, Hilario E, Dierkers A, Ngo H, Borchardt D, Neubauer TJ, Fan L, Mueller LJ, Dunn MF. Biochem. 2013; 52:6396–6411. [PubMed: 23952479]
3. Buller AR, Brinkmann-Chen S, Romney DK, Herger M, Murciano-Calles J, Arnold FH. Proc Nat Acad Sci. 2015; 112:14599–14604. [PubMed: 26553994]
4. a) Zehner S, Kotzsch A, Bister B, Süssmuth RD, Méndez C, Salas JA, van Pée K-H. Chem Biol. 2005; 12:445–452. [PubMed: 15850981] b) Zhang P, Sun X, Xu B, Bijian K, Wan S, Li G, Alaoui-Jamali M, Jiang T. Eur J Med Chem. 2011; 46:6089–6097. [PubMed: 22047643] c) Wang H, Reisman SE. Angew Chem, Int Ed. 2014; 53:6206–6210.d) Zhang J, Wu C, Sheng J, Feng X. Mol Biosyst. 2016; 12:1432–1435. [PubMed: 27008988]
5. Lehmann M, Wyss M. Curr Opin Biotech. 2001; 12:371–375. [PubMed: 11551465]
6. a) Brinkmann-Chen S, Flock T, Cahn JKB, Snow CD, Brustad EM, McIntosh JA, Meinhold P, Zhang L, Arnold FH. Proc Nat Acad Sci. 2013; 110:10946–10951. [PubMed: 23776225] b) Heel T, McIntosh JA, Dodani SC, Meyerowitz JT, Arnold FH. ChemBioChem. 2014; 15:2556–2562. [PubMed: 25294253] c) Khanal A, Yu McLoughlin S, Kershner JP, Copley SD. Mol Biol Evol. 2015; 32:100–108. [PubMed: 25246702] d) Dunn MR, Otto C, Fenton KE, Chaput JC. ACS Chem Biol. 2016; 11:1210–1219. [PubMed: 26860781]
7. Dokholyan NV. Chem Rev. 2016; 116:6463–6487. [PubMed: 26894745]
8. Nussinov R, Tsai CJ, Csermely P. Trends Pharm Sci. 2011; 32:686–693. [PubMed: 21925743]
9. Kuriyan J, Eisenberg D. Nature. 2007; 450:983–990. [PubMed: 18075577]
10. Merkl R. BMC Evol Biol. 2007; 7doi: 10.1186/1471-2148-7-59
11. For sequence and structure alignments, see supporting information.
12. Hettwer S, Sterner R. J Biol Chem. 2002; 277:8194–8201. [PubMed: 11756459]

13. Neumann CS, Fujimori DG, Walsh CT. Chem Biol. 2008; 15:99–109. [PubMed: 18291314]
14. a) Roy AD, Grüschow S, Cairns N, Goss RJM. J Am Chem Soc. 2010; 132:12243–12245. [PubMed: 20712319] b) Pathak TP, Miller SJ. J Am Chem Soc. 2013; 135:8415–8422. [PubMed: 23692563] c) Durak LJ, Payne JT, Lewis JC. ACS Catal. 2016; 6:1451–1454. [PubMed: 27274902]
15. Blaser G, Sanderson JM, Batsanov AS, Howard J. Tet Lett. 2008; 49:2795–2798.
16. Crawford IP, Ito J. Proc Nat Acad Sci. 1964; 51:390–397. [PubMed: 14171449]
17. Akgun B, Hall DG. Angew Chem, Int Ed. 2016; 55:3909–3913.
18. a) Han H, Davis ME. Bioconjugate Chem. 2013; 24:669–677.b) Pan DW, Davis ME. Bioconjugate Chem. 2015; 26:1791–1803.
19. Roy AD, Goss RJM, Wagner GK, Winn M. Chem Comm. 2008:4831–4833. [PubMed: 18830508]

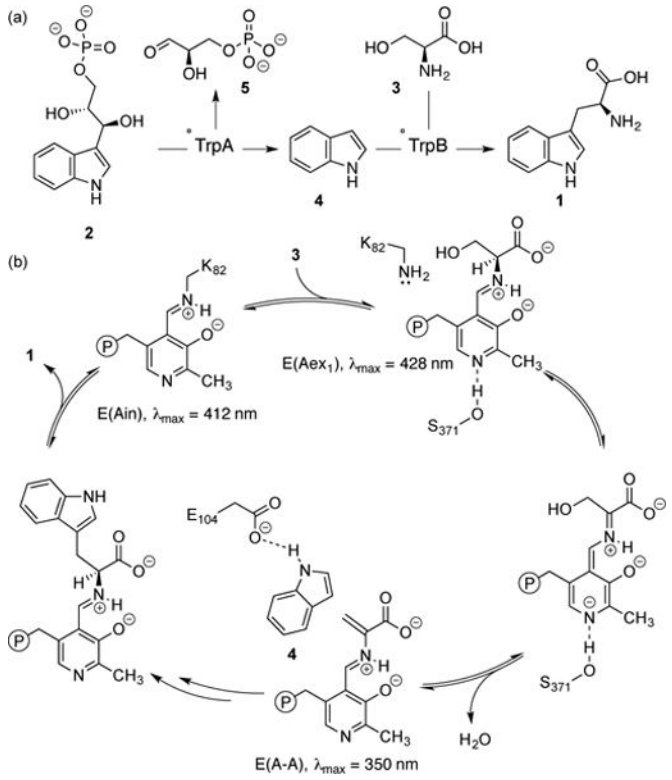

Figure 1.

Native reaction mediated by TrpS and the catalytic cycle of TrpB. (a) TrpA degrades **2** through retro-aldol cleavage to give indole (**4**) and D-glyceraldehyde (**5**). Substrate **4** then reacts with **3** to form **1**. (b) TrpB contains a pyridoxal 5′-phosphate (PLP) cofactor bound as an internal aldimine, E(Ain), which covalently binds **3** as an external aldimine, E(Aex$_1$). Subsequent deprotonation and dehydration form the amino-acrylate, E(A-A). Finally, **4** reacts with E(A-A) to form **1**.

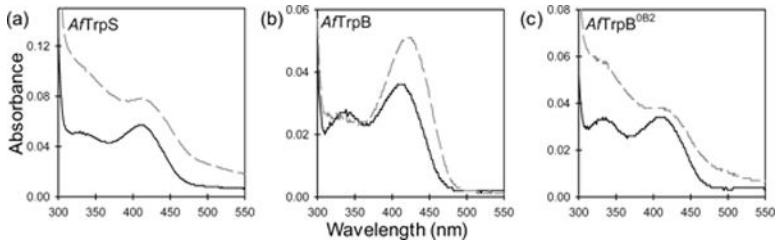

Figure 2.

UV-vis absorption spectra of (a) *Af*TrpS, (b) *Af*TrpB, and (c) *Af*TrpB^{0B2} before (solid black) and after (dashed grey) addition of L-serine.

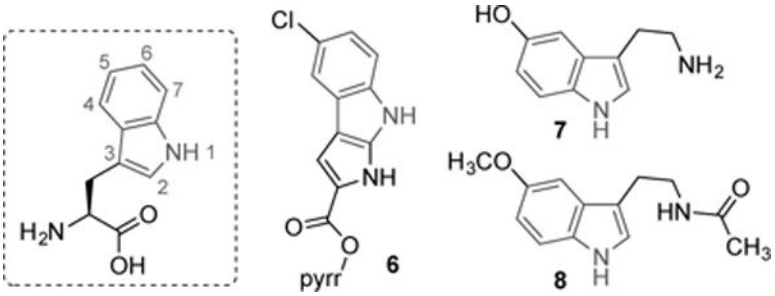

Figure 3.

Numbering of positions on the indole moiety of tryptophan and examples of natural products bearing substitution at position 5.

Table 1

Kinetic parameters of the *Pyrococcus furiosus* and *Archaeoglobus fulgidus* TrpB wild-type enzymes and 0B2 variants.[a]

Entry	Enzyme	k_{cat} (s^{-1})	K_M (μM indole)	k_{cat}/K_M ($\mu M^{-1}\ s^{-1}$ indole)
1	*Pf*TrpB^{WT}	0.31	77	4.0
2[b]	*Pf*TrpB^{0B2}	2.9	9	300
3	*Af*TrpB^{WT}	0.074	12	6.0
4[c]	*Af*TrpB^{0B2}	0.51	4.8	110

[a] Assays conducted in potassium phosphate buffer (pH 8) at 75 °C for *Pf* and 60 °C for *Af*TrpB. See SI section 5.4 for experimental details. Standard errors are in Table S1.

[b] Contains the mutations P12L, E17G, I68V, F274S, T292S, and T321A.

[c] Contains the mutations P25L, P30G, I80V, L285S, T303S, and T321A.

Table 2

Kinetic parameters of *Thermotoga maritima* TrpB variants and TrpS.[a]

Entry	Enzyme	k_{cat} (s^{-1})	K_M (μM indole)	k_{cat}/K_M ($\mu M^{-1}\ s^{-1}$ indole)
1	*Tm*TrpB^{WT}	1.28	33	39
2	*Tm*TrpB^{0B2} [b]	0.11	72	2.0
3	*Tm*TrpB^{triple} [c]	9.8	26	380
4	*Tm*TrpB^{T292S}	5.8	25	230
5	*Tm*TrpS	2.2	44	50

[a] Assays conducted in potassium phosphate buffer (pH 8) at 75 °C. See SI section 5.4 for experimental details. Standard errors are in Table S1.

[b] Contains the mutations P14L, P19G, I69V, L274S and T292S.

[c] Contains the mutations P19G, I69V, and T292S.

Table 3

Kinetic parameters of *Pyrococcus furiosus* TrpB$^{M144T\ N166D}$ and its homologs.[a]

Entry	Enzyme	k_{cat} (s^{-1})	K_M (μM indole)	k_{cat}/K_M ($\mu M^{-1}\ s^{-1}$ indole)
1	*Pf*TrpB$^{M144T\ N166D}$	0.83	42	20
2[b]	*Ec*TrpB$^{M149T\ N171D}$	0.34	18	19
3	*Tm*TrpB$^{M145T\ N167D}$	3.3	32	100
4	*Af*TrpB$^{M156T\ N178D}$	0.34	11	31

[a]Assays conducted in potassium phosphate buffer (pH 8) at 75 °C for *Pf* and *Tm*, 60 °C for *Af*, and 37 °C for *Ec*TrpB. See SI section 5.4 for experimental details. Standard errors are in Table S1.

[b]*Ec*TrpB has the following: k_{cat} = 0.16 s^{-1}; K_M = 19 μM (indole); k_{cat}/K_M = 8 $\mu M^{-1}\ s^{-1}$ (indole).

Table 4

Synthesis of 5-substituted tryptophan derivatives with *Thermotoga maritima* TrpB$^{M145T\ N167D}$[a]

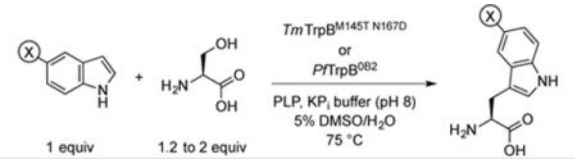

			Reaction with *Tm*TrpB$^{M145T\ N167D}$ [a]	
Entry	**X**	**Relative rate *vs* *Pf*TrpB^{0B2}**	**Isolated yield (%)[b]**	**Total turnovers[c]**
1	Cl	3.0	93	9300
2	Br	5.6	88	4400
3	NO_2	7.5	25	1250
4	CN	4.5	49	2450
5	CHO	1.9	32	1600
6	$B(OH)_2$	1.8	38[d]	1900[d]
7	OH	1.4	93[d]	9300[d]
8	CH_3	1.4	91	9100
9	OCH_3	1.5	76	7600

[a] See SI section 6 for experimental details. Standard errors are in Table S2.

[b] Reactions used either 2 equiv (entries 1–6) or 1.2 equiv (entries 7–9) of L-serine. Products isolated by chromatography with C-18 silica.

[c] Extrapolated from isolated yield based on maximum theoretical turnover number.

[d] Determined by ^{1}H NMR based on an internal standard.